

Using Nonempirical Semilocal Density Functionals and Empirical Dispersion Corrections to Model Dative Bonding in Substituted Boranes

Benjamin G. Janesko*

Department of Chemistry, Texas Christian University Fort Worth, Texas 76109

Received February 11, 2010

Abstract: Dative bonds to substituted boranes represent a challenge for the approximate exchange-correlation functionals typically used in density functional theory (DFT). Accurately modeling these bonds with DFT has usually required highly parametrized functionals, large admixtures of exact exchange, or computationally expensive double hybrids. This work shows that the nonempirical semilocal PBEsol functional, and the nonempirical semilocal PBE and TPSS functionals augmented with empirical interatomic dispersion corrections, accurately treat several representative problems in dative bonding. These methods typically surpass the MPW1K “kinetics” global hybrid previously recommended for dative bonds. This work also provides additional insights into the accuracy of the parametrized M06 functionals and indicates some deficiencies of the B97-D functional relative to PBE-D and TPSS-D. Applications to frustrated Lewis pairs illustrate the potential of these methods.

1. Introduction

Density functional theory (DFT) incorporating approximate exchange-correlation functionals has become a favored approach for modeling chemical bonding in condensed phases and medium-sized to large molecules.¹ But recent investigations^{2–4} have demonstrated that conventional functionals have severe problems treating noncovalent interactions. This has stimulated several methodological developments in DFT. These include empirical^{5,6} and nonempirical^{7,8} interatomic dispersion corrections, effective atomic core potentials to model dispersion,⁹ “fifth-rung” functionals¹⁰ incorporating approximate second-order Görling-Levy perturbation theory correlation,¹¹ and semiempirical functionals containing a large number of fitted parameters.¹²

Dative bonds (coordinate covalent bonds) to substituted boranes form an important class of relatively weak interactions. Dative bonds are strongly influenced by factors such as crystal packing^{13–15} and the interplay of substituents’ steric and electronic effects.¹⁶ Boron’s dative bonds play important roles in areas including sensing^{17,18} and supramolecular chemistry.¹⁹ Recent reports of heterolytic H₂ splitting

by “frustrated Lewis pairs” between sterically hindered boranes and Lewis bases^{20,21} has engendered much computational work on these systems.^{22–27} More broadly, dative bonding is central to transition metal chemistry, another focus of recent computational work.^{28–32}

Dative bonds to substituted boranes are a significant challenge for DFT. Standard DFT approximations, including the B3LYP^{33,34} functional used in previous investigations of borane dative bonding,^{18,35} often display qualitative and quantitative failures for these systems. Gilbert showed that B3LYP cannot reproduce accurate B–N bond lengths and bond dissociation energies for several Me_nH_{3–n}B–NMe_mH_{3–m} and (CF₃)_nH_{3–n}B–NMe_mH_{3–m} species (ref 36, “Me” = CH₃). Particularly egregious failures occurred in the sort of highly substituted, sterically congested molecules relevant to frustrated Lewis pairing. The best DFT results were obtained with the kinetics global hybrid MPW1K,³⁷ which is parametrized to reproduce reaction barrier heights. This led the author to conclude that methods designed for “incompletely bound” transition states are most appropriate for modeling dative bonds. Phillips and Cramer found that hybrid DFT functionals were required to model the bond length in F₃B–NCH and that even hybrids could not reproduce accurate B–N bond energies.³⁸ Plumley and

* To whom correspondence should be addressed; E-mail: b.janesko@tcu.edu.

Evanseck found B3LYP to be completely inadequate for modeling substituent effects in $\text{Me}_3\text{B}-\text{NMe}_n\text{H}_{3-n}$ complexes.³⁹ In these systems, competition between steric and electronic effects makes the B–N bond enthalpy increase for $n = 0 \rightarrow 2$ and then decrease at $n = 3$.⁴⁰ Of the functionals tested by the authors, only the highly parametrized Minnesota functionals¹² reproduced this experimental trend. The authors recommended the M06-2X functional, which they used extensively in a subsequent study of boron's Lewis acidity.¹⁶ Rakow and co-workers found that empirically dispersion-corrected functionals, or Minnesota functionals, were needed to treat H/Br exchange barriers in BBr_3 .⁴¹

This state of affairs is somewhat unsatisfying. Global hybrid density functionals like MPW1K and M06-2X have a relatively large computational cost due to their inclusion of exact (Hartree–Fock-type, HF) exchange.¹ Indeed, a recent MPW1K treatment of the frustrated Lewis pair and H_2 activating complex²⁰ $(\text{C}_6\text{F}_5)_3\text{B}-\text{P}(\text{tBu})_3$ [$^*\text{tBu} = \text{C}(\text{CH}_3)_3$] used the ONIOM embedding method⁴² due to computational cost.²³ The long-range part of hybrids' HF exchange is especially problematic in condensed phases,⁴³ making global hybrids inappropriate for dative bonding in nanostructures and condensed phases. Fifth-rung functionals like the B2PLYP-D⁴⁴ method recommended in ref 41 have an even higher computational expense. Additionally, while the M06 suite of functionals has demonstrated broad utility in chemistry,¹² its members have a large number of empirical parameters and appear prone to numerical errors.^{45,46}

There would be great value in a semilocal density functional that could accurately treat dative bonds in molecules, nanostructures, and condensed phases, with a low computational cost and a minimum of empiricism. ("Semilocal" density functionals model the exchange-correlation energy density and potential at each point \mathbf{r} as a function of the electron density, density gradient, and possibly the noninteracting kinetic energy density and/or density Laplacian at \mathbf{r} .¹ They are typically computationally cheaper than global hybrids.) Here, I explore two recent approximations with these characteristics: the nonempirical PBEsol generalized gradient approximation (GGA)⁴⁷ and the addition of empirical dispersion corrections⁵ to nonempirical semilocal functionals.

Surprising recent investigations have found that simple, nonempirical density functionals can accurately model the "medium-range correlation" important to noncovalent interactions. Woodrigh and co-workers showed that the local spin-density approximation (LSDA) outperformed conventional functionals for isodesmic stabilization energies of n -alkanes.³ Csonka and co-workers showed that PBEsol,⁴⁷ while designed for solids, accurately models a range of noncovalent stereoelectronic effects.⁴⁸ B3LYP gives qualitative and quantitative failures for these properties.² PBEsol has the form of the Perdew–Burke–Ernzerhof (PBE) GGA⁴⁹ and modifies two parameters to restore the correct density gradient expansion for exchange.⁴⁷

Another important development is the advent of empirical interatomic dispersion corrections⁵⁰ in DFT.^{5,6,51} Grimme's "D" corrections add a damped, molecular-mechanics-type

R^{-6} internuclear attraction to a DFT calculation. These provide a straightforward route to improving noncovalent interactions in large systems.⁵¹ They have been successfully applied to a few problems in dative bonding.^{22,26,41,52,53} However, much of that work focused on dispersion-corrected double hybrids whose computational expense is comparable to MP2. To date, a systematic study of "D" corrections for dative bonding has not appeared.

This work benchmarks the methods of refs 3, 48, and 51 for dative bonds to substituted boranes. I test the nonempirical LSDA and PBEsol functionals, and the addition of empirical dispersion corrections to the nonempirical PBE and TPSS functionals. These methods significantly improve upon conventional global hybrids, approaching the accuracy of M06-2X at reduced computational cost. Selected results for the entire M06 suite of functionals provide new insight into these methods' success. Conversely, tests of the dispersion-corrected B97-D functional indicate that its accurate performance in other areas⁵¹ does not carry over to dative bonds.

2. Computational Details

All calculations use a development version of the Gaussian suite of programs.⁵⁴ Unless noted otherwise, calculations use the correlation-consistent aug-cc-pVTZ basis set⁵⁵ or the large Pople basis 6-311++G(3df,2p).⁵⁶ Binding energies and enthalpies include counterpoise corrections for basis set superposition error.⁵⁷ Self-consistent field (SCF) calculations converge the energy to at least 10^{-8} Hartree with corresponding thresholds for geometry calculations (Gaussian keywords "SCF=Tight" and "Geom=Tight"). DFT numerical integrations use at least an "UltraFine" integration grid with 99 radial and 590 angular points per atom. Unless noted otherwise, energies are evaluated with geometries optimized using the corresponding method. Counterpoise corrections are not included during the geometry optimizations. All calculations treat isolated molecules, with no corrections for solvation or crystal packing effects. Open-shell systems are treated spin-unrestricted. Other computational details are taken from the literature (vide infra).

This work focuses on nonempirical and dispersion-corrected semilocal exchange-correlation functionals. These include the local spin-density approximation LSDA (Vosko–Wilk–Nusair correlation functional V, ref 58), the Perdew–Burke–Ernzerhof (PBE) GGA,⁴⁹ the Tao–Perdew–Staroverov–Scuseria (TPSS) meta-GGA,⁵⁹ and the PBEsol GGA.⁴⁷ PBE-D and TPSS-D use Grimme's empirical interatomic dispersion correction.^{5,6,51} Scale factors $s_6 = 0.75$ (PBE-D) and $s_6 = 1.00$ (TPSS-D) are taken from ref 6. The empirical B97-D functional is also tested.⁶ Selected systems are tested for the entire M06 suite of functionals: the semilocal M06-L meta-GGA,⁶⁰ the M06 hybrid meta-GGA incorporating 27% HF exchange,¹² the M06-2X hybrid with 54% HF exchange,¹² and the "density functional for spectroscopy" M06-HF with 100% HF exchange.⁶¹ While M06-2X is recommended for problems like dative bonding,¹² results from the entire suite can provide interesting insights into these functionals. The B3PW91,³³ B3LYP,³⁴ and MPW1K³⁷ global hybrid functionals are included for comparisons to previous work.

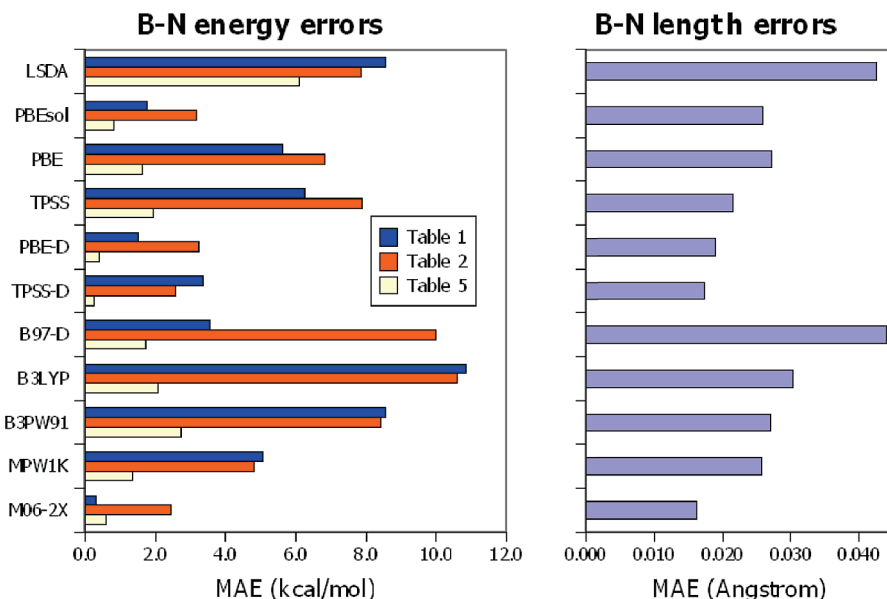


Figure 1. Cumulative statistical errors in B–N bond strengths (left) and bond lengths (right). The left panel plots the MAE in B–N bond energies/enthalpies from Tables 1, 2, and 5. The right panel plots the MAE in B–N bond lengths from Table 4.

Table 1. B–N Bond Enthalpies at 373 K (kcal/mol) for Methyl Substituted Amine Boranes^a

method	Me ₃ B–NH ₃	Me ₃ B–NH ₂ Me	Me ₃ B–NHMe ₂	Me ₃ B–NMe ₃	MAE
exptl	–13.8 ± 0.3	–17.6 ± 0.2	–19.3 ± 0.3	–17.6 ± 0.2	
LSDA	–22.6	–27.1	–27.6	–25.2	8.6
PBEsol	–16.6	–19.7	–19.1	–15.7	1.8
PBE	–11.4	–13.9	–12.4	–8.1	5.6
TPSS	–11.0	–13.0	–11.6	–7.7	6.3
PBE-D	–15.2	–19.7	–20.7	–18.8	1.5
TPSS-D	–16.0	–20.9	–22.7	–22.2	3.4
B97-D	–9.8	–14.4	–15.6	–14.3	3.6
B3LYP	–6.8	–8.8	–7.0	–2.4	10.8
B3PW91	–9.1	–11.0	–9.2	–4.8	8.6
MPW1K	–11.9	–14.2	–12.9	–9.1	5.1
M06-L	–9.7	–13.1	–13.3	–11.5	5.2
M06	–10.3	–14.0	–14.6	–12.5	4.2
M06-2X	–14.1	–18.3	–19.2	–17.8	0.3
M06-HF	–20.0	–24.9	–26.7	–26.2	7.4

^a Counterpoise-corrected 6-311++G(3df,2p) calculations, experimental results from ref 39.

3. Results

Figure 1 presents a cumulative picture of the results. The figure shows mean absolute errors (MAE) in bond energies/enthalpies and bond lengths for several sets of B–N dative bonds. To summarize, the dispersion-corrected PBE-D and TPSS-D functionals give very accurate B–N dissociation energies and bond lengths. These methods surpass the previously recommended MPW1K functional and approach the accurate M06-2X functional. PBEsol is also accurate for B–N dissociation energies, though it tends to underestimate bond lengths. The remainder of this section details the individual studies in Figure 1 and discusses applications to larger systems.

3.1. Bond Strengths of Substituted Amine Boranes.

References 39 and 40 studied the B–N bond enthalpies of four Me₃B–NMe_nH_{3–n} derivatives. These references tested the B3LYP, MPW1K, MPWB1K, MPWB95, and M05/M06 density functionals. The experimental trend, in which the B–N dative bond strengthens for *n* from 0–2 and

decreases at *n* = 3, was only reproduced by the M05-2X, M06, and M06-2X functionals.

Table 1 shows new calculations on these Me₃B–NMe_nH_{3–n} derivatives. The calculations in Table 1 follow refs 39 and 40, evaluating binding enthalpies at 373 K using B3LYP/6-31G(d) thermal corrections rescaled by 0.9941. Counterpoise-corrected thermal corrections were taken from ref 39. The B3LYP, MPW1K, and M06-2X results in Table 1 reproduce ref 40 to within ±0.1 kcal/mol. The basis set is relatively saturated: all methods except for the Minnesota functionals give counterpoise corrections < 1 mH.

The most striking results in Table 1 involve the relative binding enthalpies. While LSDA overbinds, it correctly predicts that the bond enthalpies strengthen for *n* from 0 to 2 and decrease at *n* = 3. None of the DFT methods tested in ref 39 reproduced this trend. PBEsol nearly reproduces the trend and also gives absolute bond enthalpies that significantly improve on LSDA. This is consistent with previous observations of medium-range correlation in LSDA³ and

Table 2. B–N Bond Dissociation Energies (kcal/mol) for Trifluoromethyl Substituted Amine Boranes^a

method	(CF ₃)H ₂ B–NH ₃	(CF ₃) ₂ HB–NH ₃	(CF ₃) ₃ B–NH ₃	MAE
reference	–40.4	–52.6	–62.6	
LSDA	–51.7	–60.1	–67.4	7.9
PBEsol	–44.3	–51.8	–57.8	3.2
PBE	–38.3	–45.7	–51.1	6.8
TPSS	–36.7	–44.6	–50.6	7.9
PBE-D	–41.0	–49.7	–56.4	3.2
TPSS-D	–40.3	–50.0	–57.6	2.6
B97-D	–33.6	–42.6	–49.4	10.0
B3LYP	–33.5	–42.0	–48.3	10.6
B3PW91	–36.1	–44.1	–50.1	8.4
MPW1K	–38.6	–47.8	–54.8	4.8
M06-2X	–39.2	–49.9	–59.1	2.5

^a Counterpoise-corrected 6-311++G(3df,2p) calculations. Reference MP2/6-311++G(d,p) results are from ref 36.

PBEsol.⁴⁸ These results are not a basis set artifact: PBEsol calculations in the aug-cc-pVTZ basis set return bond enthalpies within ± 0.1 kcal/mol of those in Table 1. PBEsol significantly improves upon the MPW1K functional recommended in ref 36 and approaches the accuracy of M06-2X.

Another important result in Table 1 is the success of empirical dispersion corrections. PBE and TPSS do not reproduce the absolute bond enthalpies of Me₃B–NMe_nH_{3–n} or the trend with increasing *n*. But adding empirical “-D” dispersion corrections to these nonempirical functionals dramatically improves their performance. PBE-D and TPSS-D both reproduce the experimental trend, and PBE-D gives overall accuracy comparable to PBEsol and approaching M06-2X. This result agrees with ref 62, which showed that PBE-D reproduces MP2 benchmarks for H₃B–PH₃ and Me₃B–PMe₃.

The B97-D GGA, whose empirical functional form was explicitly parametrized to complement its dispersion correction,⁶ underestimates B–N bond strengths. This is unlikely to be a basis set artifact: geometry-optimized B97-D/aug-cc-pVTZ calculations give counterpoise-corrected dissociation enthalpies within ± 0.1 kcal/mol of those in Table 1. B97-D also significantly overestimates B–N dative bond lengths (vide infra). Note in this context that ref 22 showed B97-D significantly underestimates the B–P dative bond strength in a cyclic intramolecular phosphane–borane adduct.⁶³

Table 1 also shows that the entire M06 series of functionals reproduces the experimental trend in binding enthalpies. While the absolute binding enthalpies vary with the fraction of HF exchange, all four functionals appear to give a reasonable account of the medium-range correlation that produces this trend. This indicates that the parametrization procedure for these functionals is quite robust.

Table 2 shows the B–N bond dissociation energies of trifluoromethyl substituted amine boranes (CF₃)_nH_{3–n}B–NH₃. These compounds were studied in ref 36, which concluded that conventional DFT functionals failed to reproduce the steep increase in bond energy upon fluorination. The best DFT results were obtained with the MPW1K kinetics global hybrid. This was justified by the observation that MPW1K

is designed to model transition states, and by the claim that “incompletely bound” transition states mimic datively bonded systems.³⁶

Calculations in Table 2 use the 6-311++G(3df,2p) basis. They include HF/6-31+G(d) zero-point energy corrections empirically rescaled by 0.9153, following ref 36. The counterpoise corrections are somewhat larger than in Table 1, though they are < 2 mH in all but a few systems. The B3LYP, B3PW91, and MPW1K bond energies are a few kilocalories per mole smaller than the corresponding non-counterpoise-corrected 6-311++G(d,p) values in ref 36. Aug-cc-pVTZ calculations give counterpoise-corrected PBE-D, B97-D, and M06-2X dissociation energies within ± 0.2 kcal/mol of Table 2. This indicates that the results are unlikely to be a basis set artifact.

The most important result in Table 2 is the accuracy of the PBEsol GGA and the dispersion-corrected PBE-D and TPSS-D functionals. As in Table 1, these methods all improve upon MPW1K at this level of theory and approach M06-2X. Table 2 also supports refs 40 and 41 in demonstrating that M06-2X is very accurate for these systems. As in Table 1, B97-D significantly underbinds relative to PBE-D and TPSS-D.

The other nonempirical functionals in Table 2 perform less well. LSDA strongly overbinds, as expected, and PBE and TPSS tend to underbind. But even these functionals, like BPW91, outperform B3LYP for this system.

The non-counterpoise-corrected MPW1K/6-311++G(d,p) results reported in ref 36 are better than any functionals in Table 2 in reproducing the non-counterpoise-corrected MP2/6-311++G(d,p) reference values. This is partly an artifact of a cancellation between finite basis set error and basis set superposition error (BSSE). Omitting the counterpoise correction gives PBEsol, PBE-D, TPSS-D, and M06-2X MAE of 2.7, 2.8, 2.0, and 1.7 kcal/mol vs the reference values in Table 2. These are comparable to the 1.9 kcal/mol MAE reported for MPW1K in ref 36. Additionally, new counterpoise-corrected MP2/aug-cc-pVTZ calculations at MP2/cc-pVTZ geometries give binding energies of –37.9, –48.6, and –57.3 kcal/mol for the three molecules in Table 2. These are 3–5 kcal/mol below the corresponding noncounterpoise-corrected MP2/6-311++G(2d,2p) values in ref 36. Comparing the calculations in Table 2 to these new reference values gives PBEsol, PBE-D, TPSS-D, MPW1K, and M06-2X MAE of 3.4, 1.7, 1.4, 1.3, and 1.4 kcal/mol. PBE-D, TPSS-D, and M06-2X are again comparable to MPW1K.

The accurate performance of PBEsol, PBE-D, and TPSS-D in Tables 1 and 2 suggests that accurate performance for “incompletely bound” transition states is not necessary for modeling dative bonds. Unlike MPW1K and M06-2X, these functionals contain no HF exchange and cannot adequately predict gas-phase reaction barriers. This is illustrated in Table 3, which shows statistical errors in the BH6 set of representative hydrogen-transfer reaction barrier heights.⁶⁴ Geometries for this data set are from ref 64, and spin–orbit corrections are from ref 65. PBEsol’s poor performance for reaction barriers was also shown in ref 66. I suggest that a method’s description of medium-range correlation, and not

Table 3. Mean Errors ME and Mean Absolute Errors MAE (kcal/mol) in BH6 Hydrogen-Transfer Reaction Barrier Heights^a

method	ME	MAE
LSDA	-17.9	17.9
PBEsol	-12.8	12.8
PBE	-9.4	9.4
PBE-D	-9.8	9.8
TPSS-D	-8.8	8.8
B97-D	-6.0	6.3
MPW1K	-1.1	1.4
M06-2X	-0.7	1.2

^a Aug-cc-pVTZ calculations.**Table 4.** Equilibrium B–N Bond Lengths (Å) for Methyl Substituted Amine Boranes^a

method	H ₃ B–NH ₃	H ₃ B–NMe ₃	Me ₃ B–NMe ₃	MAE
exptl	1.658(2)	1.656(2)	1.70(1)	
LSDA	1.606	1.599	1.682	0.043
PBEsol	1.628	1.621	1.714	0.026
PBE	1.647	1.642	1.758	0.027
TPSS	1.663	1.653	1.757	0.021
PBE-D	1.653	1.637	1.734	0.019
TPSS-D	1.672	1.645	1.728	0.017
B97-D	1.692	1.665	1.790	0.044
B3LYP	1.657	1.651	1.785	0.030
B3PW91	1.644	1.637	1.749	0.027
MPW1K	1.632	1.625	1.722	0.026
M06-2X	1.648	1.638	1.722	0.016

^a 6-311++G(3df,2p) calculations. Gas-phase experimental values are taken from ref 36.

its treatment of transition states, is the decisive factor for modeling dative bonding.

3.2. Geometries of Substituted Amine Boranes. The B–N bond length in amine boranes and related compounds⁶⁷ is sensitive to crystal packing effects,^{13–15} making it inappropriate to compare gas-phase calculations with experimental crystal structures. Reference 36 collected gas-phase experimental structures for three substituted amine boranes. That reference concluded that, as for bond energies, MPW1K provided the most accurate treatment of bond lengths.

Table 4 shows how several DFT methods reproduce these experiments. The table shows the equilibrium B–N bond lengths from 6-311++G(3df,2p) calculations on H₃B–NH₃, H₃B–NMe₃, and Me₃B–NMe₃. The B3LYP and MPW1K results are within 0.01 Å of the 6-311++G(d,p) results in ref 36. Test calculations indicate that the results are unlikely to be a basis set artifact. Aug-cc-pVTZ calculations with PBEsol, PBE-D, B97-D, and M06-2X give bond lengths 0.002 Å longer than those in Table 4 for H₃B–NH₃, and within ±0.001 Å of those in Table 4 for the other two molecules.

The accurate performance of PBE-D, TPSS-D, and M06-2X for dative bond energies carries over to bond lengths. These methods provide the most accurate results in Table 4. All three outperform both the MPW1K/6-311++G(3df,2p) geometries in Table 4 and the MPW1K/6-311++G(d,p) geometries reported in ref 36. While TPSS gives the lowest MAE among nonempirical functionals, it overestimates the bond length of the most highly substituted compound.

Table 5. Equilibrium B–N Bond Lengths (*R*(B–N), Å) and Counterpoise-Corrected B–N Dissociation Energies (DE, kcal/mol) for HCN–BF₃^a

method	<i>R</i> (B–N)	DE
reference	2.472	-5.6
LSDA	1.729	-11.7
PBEsol	1.820	-6.4
PBE	2.410	-4.0
TPSS	2.243	-3.7
PBE-D	2.362	-5.2
TPSS-D	2.234	-5.3
B97-D	2.682	-3.9
B3LYP	2.535	-3.5
B3PW91	2.465	-2.9
MPW1K	2.323	-4.2
M06-2X	2.385	-6.2

^a Aug-cc-pVTZ calculations without zero-point or thermal corrections. Reference MC-QCISD results are from ref 38.

(Similar errors for conventional DFT functionals were shown in ref 36.) This overestimation is improved by the “-D” dispersion correction, illustrating the importance of medium-range correlation in this highly substituted system.

As mentioned above, B97-D overestimates all of the B–N bond lengths, giving the largest MAE of any tested functional. The accurate PBE-D and TPSS-D results suggest that this is not a failure of the dispersion correction but a limitation of the B97-D parametrization. This result rationalizes B97-D’s poor performance for the bond energies/enthalpies in Tables 1 and 2. (Here, it is appropriate to reiterate B97-D’s accuracy for other systems.⁵¹)

3.3. Bond Strength and Bond Length in HCN–BF₃. Reference 38 characterized the gas-phase structure and B–N binding energies of the HCN–BF₃ dative bond. Comparisons to accurate MC-QCISD or MG3 results showed that, while some conventional functionals gave reasonable geometries, all tended to underestimate bond energies. Table 5 shows HCN–BF₃ B–N bond lengths and dissociation energies for the functionals considered here. These counterpoise-corrected aug-cc-pVTZ results differ slightly from the non-counterpoise-corrected results in ref 38. The counterpoise corrections are <1 mH, indicating that the basis set is reasonably saturated.

The results in Table 5 reiterate those in Tables 1–4. PBE-D, TPSS-D, and M06-2X accurately model both the bond length and the dissociation energy, providing significant improvements over the B3PW91, B3LYP, and MPW1K global hybrids. PBEsol strikes a balance between the overbinding of LSDA and the underbinding of PBE, though (as in Table 4), it underestimates the dative bond length. Unlike the other dispersion-corrected functionals, B97-D severely overestimates the bond length and underestimates the bond energy. The spread in bond length errors is much larger than in Table 4, indicating that the bond has a shallow minimum.

3.4. Basis Set Dependence. Previous studies have indicated that dative bonds strongly depend on the one-electron basis set.^{36,38} Given this, it is of interest to test the basis set dependence of the density functionals used here. Figure 2 shows the basis set dependence of a representative system: the equilibrium B–N bond length and counterpoise-corrected

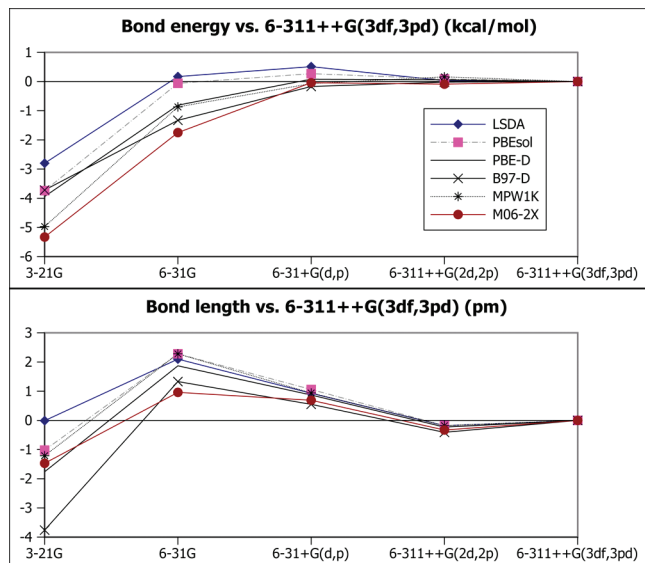


Figure 2. Basis set dependence of B–N bond energy (top) and bond length (bottom) in $(\text{CH}_3)_3\text{B}-\text{N}(\text{CH}_3)_3$. Counterpoise-corrected geometry-optimized calculations. Results are relative to the large 6-311++G(3df,3pd) basis set.

bond energy of $\text{Me}_3\text{B}-\text{NMe}_3$. The figure shows the bond energy (top) and bond length (bottom) evaluated in a variety of basis sets. Results are evaluated relative to the large 6-311++G(3df,3pd) basis set. All of the methods tested here have roughly comparable basis set dependence. This is encouraging given previous reports⁴¹ of large basis set effects for the Minnesota functionals. All methods show a rather large basis set dependence for bond lengths. However, bond lengths and bond energies are fairly well converged in the “desert island double- ζ ”⁶⁸ 6-31+G(d,p) basis set. This basis set should provide a reasonable compromise for modeling larger systems such as frustrated Lewis pairs.

3.5. Application to Larger Systems. One goal of this work is to find computationally inexpensive DFT methods for modeling the large, sterically congested substituted boranes relevant to frustrated Lewis pairing.²¹ An important drawback of conventional semilocal and hybrid density functionals is that their errors tend to increase with system size. For example, the mean absolute error in B3LYP enthalpies of formation increases from 3.08 kcal/mol for the G2/97 test set of 147 small molecules, to 8.21 kcal/mol for the 75 larger molecules in the G3-3 set.⁶⁹ However, the parametrized and dispersion-corrected functionals tested here were constructed to provide comparable accuracy for both small and large systems. These functionals’ accuracy for large systems has been amply demonstrated in the literature. Reference 48 showed that M05-2X, PBEsol, and empirically dispersion-corrected functionals accurately predicted isomerization energies of large organic molecules. Comparable performance for M06-2X was demonstrated in ref 70. Reference 71 showed that dispersion-corrected semilocal functionals accurately predict intermolecular interaction energies for a data set containing both small (e.g., $(\text{H}_2\text{O})_2$) and relatively large (e.g., phenylalanine-tryptophan) biologically relevant complexes.⁴ (Further applications of empirical dispersion corrections to large molecules are reviewed in ref

Table 6. Equilibrium B–P Bond Lengths ($R(\text{B}-\text{P})$, Å) and Counterpoise-Corrected B–P Bond Energies (DE, kcal/mol) for $(\text{F}_5\text{C}_6)_3\text{B}-\text{P}(\text{t-Bu})_3$ and $(\text{F}_3\text{C})_3\text{B}-\text{P}(\text{t-Bu})_3$ ^a

method	$(\text{F}_3\text{C})_3\text{B}-\text{P}(\text{t-Bu})_3$		$(\text{F}_5\text{C}_6)_3\text{B}-\text{P}(\text{t-Bu})_3$	
	DE	$R(\text{B}-\text{P})$	DE	$R(\text{B}-\text{P})$
reference	−69	2.163	−19	3.838
LSDA	−49	2.118	−12	3.476
PBEsol	−31	2.178	−1	4.123
PBE	−27	2.184	0	4.700
PBE-D	−45	2.133	−11	3.809
B97-D	−38	2.168	−10	3.963
MPW1K	−30	2.143	1	4.975
M06-2X	−44	2.122	−10	3.722

^a 6-31+G(d,p) calculations, reference values from ref 23.

51.) Reference 70 showed that M06-2X gives a mean unsigned error of only 2.86 kcal/mol for the aforementioned G3-3 set of larger molecule thermochemistries, as well as a mean unsigned error of 5.7 kcal/mol (vs 26.2 kcal/mol for B3LYP) for 14 “large molecule” (>55 valence electrons) atomization energies. Given this, it seems reasonable to expect that the accurate performance shown above for M06-2X and PBE-D will carry over to larger molecules.

Table 6 illustrates some of the methods tested here for two relatively large systems. $(\text{F}_5\text{C}_6)_3\text{B}-\text{P}(\text{t-Bu})_3$ ($\text{t-Bu} = \text{C}(\text{CH}_3)_3$) is a weakly bound frustrated Lewis pair (ref 21) that performs heterolytic H_2 splitting under relatively mild conditions.²⁰ $(\text{F}_3\text{C})_3\text{B}-\text{P}(\text{t-Bu})_3$ was predicted in ref 23 to have a B–P dissociation energy of 69 kcal/mol, which is very high for a “weak” dative bond. These systems were modeled in ref 23 using the composite three-layer ONIOM G2R3 method at two-layer ONIOM MPW1K geometries.^{72,73}

Table 6 presents 6-31+G(d,p) calculations of the equilibrium B–P bond length and counterpoise-corrected bond energy of $(\text{F}_5\text{C}_6)_3\text{B}-\text{P}(\text{t-Bu})_3$ and $(\text{F}_3\text{C})_3\text{B}-\text{P}(\text{t-Bu})_3$. Calculations include HF/3-21G zero-point corrections rescaled by 0.9207, following ref 23. The maximum counterpoise corrections are 2.8 kcal/mol for $(\text{F}_3\text{C})_3\text{B}-\text{P}(\text{t-Bu})_3$ and 2.3 kcal/mol for $(\text{F}_5\text{C}_6)_3\text{B}-\text{P}(\text{t-Bu})_3$, indicating that the basis set is moderately saturated. PBE-D/6-311++G(2d,2p) calculations at the PBE-D/6-31+G(d,p) geometries give counterpoise-corrected binding energies within ± 0.1 kcal/mol of those in Table 6, providing further confidence in the results.

Interestingly, M06-2X and PBE-D provide similar geometric and energetic predictions for both systems in Table 6. The bond energies are significantly smaller than the high-level composite values reported in ref 23. This appears to arise from basis set superposition error in the composite method. Reference 23 reported BSSEs of 18.2 and 10.6 kcal/mol in the composite method’s dative bond dissociation energies for $(\text{F}_3\text{C})_3\text{B}-\text{PPh}_3$ and $(\text{F}_5\text{C}_6)_3\text{Al}-\text{P}(\text{CH}_3)_3$ and estimated an average 14–15 kcal/mol BSSE for all molecules tested. Simply transferring the $(\text{F}_3\text{C})_3\text{B}-\text{PPh}_3$ BSSE to $(\text{F}_3\text{C})_3\text{B}-\text{P}(\text{t-Bu})_3$ and the $(\text{F}_5\text{C}_6)_3\text{Al}-\text{P}(\text{CH}_3)_3$ BSSE to $(\text{F}_5\text{C}_6)_3\text{B}-\text{P}(\text{t-Bu})_3$ gives dissociation energies within ~ 6 and ~ 3 kcal/mol of the respective PBE-D values. Additional insight into BSSE may be obtained from the B–N dissociation energy of $(\text{CF}_3)_3\text{B}-\text{N}(\text{CH}_3)_3$, a somewhat smaller molecule treated in ref 23. That reference reported dissociation energies of 67 kcal/mol for noncounterpoise-corrected

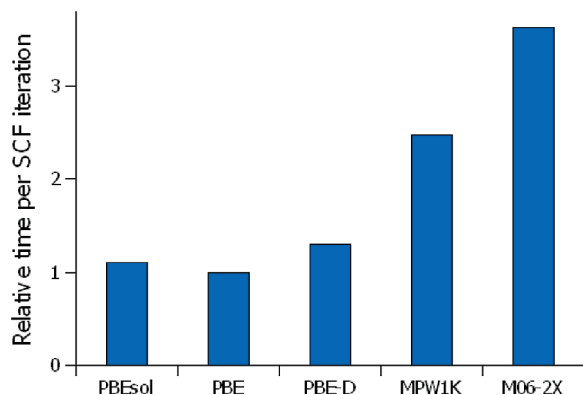


Figure 3. Average time per SCF iteration for a single self-consistent 6-31+G(d,p) total energy calculation on $(F_5C_6)_3B-P(t-Bu)_3$. Timings are reported relative to PBE.

MP2/6-311++G(d,p) and 64 kcal/mol for the composite method. New MP2/6-311++G(d,p) calculations give a non-counterpoise-corrected dissociation energy of 66.47 kcal/mol, and a corresponding counterpoise-corrected dissociation energy of only 52 kcal/mol. Counterpoise-corrected MPW1K, PBE-D, and M06-2X calculations give dissociation energies of 49, 58, and 63 kcal/mol, respectively. PBE-D and M06-2X binding energies are somewhat larger than MP2, which is reasonable given that MP2 should underbind in this relatively small basis set.

As in Tables 1–5, PBE and MPW1K both predict dative bonds that are significantly weaker than M06-2X or PBE-D. The relatively weak PBEsol bond in $(F_5C_6)_3B-P(t-Bu)_3$ is somewhat surprising and suggests that medium-range correlation plays an unusually large role. The 4.975 Å MPW1K bond length in $(F_5C_6)_3B-P(t-Bu)_3$ is significantly longer than the 3.838 Å MPW1K/ONIAM bond length obtained in ref 23. This difference may result from the small (3-21G) ligand basis set used in ref 23. MPW1K calculations in the 6-31G(d) and 3-21G basis sets yield B–P bond lengths of 4.388 and 3.631 Å, respectively, for this system.

The $(F_5C_6)_3B-P(t-Bu)_3$ molecule shown in Table 6 also provides an opportunity to illustrate the relative computational expense of these methods. Figure 3 shows the average time per SCF cycle in a single-point 6-31+G(d,p) calculation on this system.⁷⁴ Of course, computational times strongly depend on details of the implementation and hardware, and these results should be taken as no more than a rough guide. But this reiterates that hybrids like MPW1K and M06-2X typically have a computational cost significantly higher than dispersion-corrected semilocal functionals.

4. Conclusions

Previous DFT studies of dative bonds to substituted boranes indicated systematic failures of standard approximate exchange-correlation functionals. The results presented here show that the nonempirical PBEsol GGA gives accurate energies and reasonable (though overbound) geometries for a range of dative bonds. This extends previous indications⁴⁸ that PBEsol, which was built to model condensed phases, can mimic chemically important “medium-range” electron correlation effects. Adding empirical dispersion corrections to the nonempirical PBE and TPSS functionals gives even

higher overall accuracy, while maintaining a modest computational cost. These contrast with the dispersion-corrected B97-D GGA, which significantly overestimates B–N bond lengths. These results also support and extend previous indications^{40,41} that the Minnesota functionals are very accurate for these systems. The entire suite of M06 functionals shows particularly notable accuracy for relative binding trends. However, applications to larger systems reiterate the value of the computationally cheap “-D” methods.

These results should extend the options available for modeling dative bonds in large systems. Dispersion-corrected nonempirical semilocal functionals offer the best overall balance between cost and accuracy, with only a modest degree of empiricism. M06-2X provides the highest numerical accuracy in systems where global hybrids are affordable.

Acknowledgment. This work was supported by a startup grant from Texas Christian University.

References

- (1) Scuseria, G. E.; Staroverov, V. N. Progress in the development of exchange-correlation functionals. In *Theory and Applications of Computational Chemistry: The First 40 Years*; Dykstra, C. E., Frenking, G., Kim, K. S., Scuseria, G. E., Eds.; Elsevier: Amsterdam, 2005; pp 669–724.
- (2) Grimme, S. *Angew. Chem., Int. Ed.* **2006**, *45*, 4460.
- (3) Woodrich, M. D.; Corminbeuf, C.; Schleyer, P. v. R. *Org. Lett.* **2006**, *8*, 3631.
- (4) Jurečka, P.; Šponer, J.; Černý, J.; Hobza, P. *Phys. Chem. Chem. Phys.* **2006**, *8*, 1985.
- (5) Grimme, S. *J. Comput. Chem.* **2004**, *25*, 1463.
- (6) Grimme, S. *J. Comput. Chem.* **2006**, *27*, 1787.
- (7) Becke, A. D.; Johnson, E. R. *J. Chem. Phys.* **2005**, *122*, 154104.
- (8) Tkatchenko, A.; Scheffler, M. *Phys. Rev. Lett.* **2009**, *102*, 073005.
- (9) von Lilienfeld, O. A.; Tavernelli, I.; Rothlisberger, U.; Sebastiani, D. *Phys. Rev. Lett.* **2004**, *93*, 153004.
- (10) Perdew, J. P.; Schmidt, K. Jacob’s Ladder of Density Functional Approximations for the Exchange-Correlation Energy. In *Density Functional Theory and its Application to Materials*; Van Doren, V., Van Alsenoy, C., Geerlings, P., Eds.; American Institute of Physics, 2001; pp 1–20.
- (11) Grimme, S. *J. Chem. Phys.* **2006**, *124*, 034108.
- (12) Zhao, Y.; Truhlar, D. G. *Theor. Chem. Acc.* **2008**, *120*, 215.
- (13) Thorne, L. R.; Suenram, R. D.; Lovas, F. J. *J. Chem. Phys.* **1983**, *78*, 167.
- (14) Bühl, M.; Steinke, T.; von Ragu’e Schleyer; Boese, R. *Angew. Chem., Int. Ed.* **1991**, *30*, 1160.
- (15) Finze, M.; Bernhardt, E.; Terheiden, A.; Berkei, M.; Willner, H.; Christen, D.; Oberhammer, H.; Aubke, F. *J. Am. Chem. Soc.* **2002**, *124*, 15385.
- (16) Plumley, J. A.; Evanseck, J. D. *J. Phys. Chem. A* **2009**, *113*, 5985.
- (17) James, T. D.; Sandanayake, K. R. A. S.; Shinkai, S. *Angew. Chem. Intl. Ed.* **1996**, *35*, 1910.
- (18) Zhu, L.; Shabbir, S. H.; Gray, M.; Lynch, V. M.; Sorey, S.; Anslyn, E. V. *J. Am. Chem. Soc.* **2006**, *128*, 1222.

- (19) Christinat, N.; Scopelliti, R.; Severin, K. *J. Org. Chem.* **2007**, 72, 2192.
- (20) Welch, G. C.; Stephan, D. W. *J. Am. Chem. Soc.* **2007**, 129, 1880.
- (21) Stephan, D. W. *Org. Biomol. Chem.* **2008**, 6, 1535.
- (22) Spies, P.; Erker, G.; Kehr, G.; Bergander, K.; Fröhlich, R.; Grimme, S.; Stephan, D. W. *Chem. Commun.* **2007**, 5072.
- (23) Gille, A. L.; Gilbert, T. M. *J. Chem. Theory Comput.* **2008**, 4, 1681.
- (24) Geier, S. J.; Gilbert, T. M.; Stephan, D. W. *J. Am. Chem. Soc.* **2008**, 130, 12632.
- (25) Sumerin, V.; Schultz, F.; Nieger, M.; Atsumi, M.; Wang, C.; Leskela, M.; Pyykko, P.; Repo, T.; Rieger, B. *J. Organomet. Chem.* **2009**, 694, 2654.
- (26) Mömmling, C. M.; Otten, E.; Kehr, G.; Fröhlich, R.; Grimme, S.; Stephan, D. W.; Erker, G. *Angew. Chem., Int. Ed.* **2009**, 48, 6643.
- (27) Rokob, T. A.; Hamza, A.; Pápai, I. *J. Am. Chem. Soc.* **2009**, 131, 10701.
- (28) Hyla-Krispin, I.; Grimme, S. *Organometallics* **2004**, 23, 5581.
- (29) Furche, F.; Perdew, J. P. *J. Chem. Phys.* **2006**, 124, 044103.
- (30) Bühl, M.; Kabrede, H. *J. Chem. Theory Comput.* **2006**, 2, 1282.
- (31) Becke, A. D.; Johnson, E. R. *J. Chem. Phys.* **2007**, 127, 124108.
- (32) Jiménez-Hoyos, C. A.; Janesko, B. G.; Scuseria, G. E. *J. Phys. Chem. A* **2009**, 113, 11742.
- (33) Becke, A. D. *J. Chem. Phys.* **1993**, 98, 5648–5652.
- (34) Stephens, P. J.; Devlin, F. J.; Chabalowski, C. F.; Frisch, M. J. *J. Phys. Chem.* **1994**, 98, 11623–11627.
- (35) Staubitz, A.; Besora, M.; Harvey, J. N.; Manners, I. *Inorg. Chem.* **2008**, 47, 5910.
- (36) Gilbert, T. M. *J. Phys. Chem. A* **2004**, 108, 2550.
- (37) Lynch, B. J.; Fast, P. L.; Harris, M.; Truhlar, D. G. *J. Phys. Chem. A* **2000**, 104, 4811–4815.
- (38) Phillips, J. A.; Cramer, C. J. *J. Chem. Theory Comput.* **2005**, 1, 827.
- (39) Plumley, J. A.; Evanseck, J. D. *J. Phys. Chem. A* **2007**, 111, 13472.
- (40) Plumley, J. A.; Evanseck, J. D. *J. Chem. Theory Comput.* **2008**, 4, 1249.
- (41) Rakow, J. R.; Tüllmann, S.; Holthausen, M. C. *J. Phys. Chem. A* **2009**, 113, 12035.
- (42) Svensson, M.; Humbel, S.; Froese, R. D. J.; Matsubara, T.; Sieber, S.; Morokuma, K. *J. Phys. Chem.* **1996**, 100, 19357.
- (43) Janesko, B. G.; Henderson, T. M.; Scuseria, G. E. *Phys. Chem. Chem. Phys.* **2009**, 11, 443.
- (44) Schwalbe, T.; Grimme, S. *Phys. Chem. Chem. Phys.* **2007**, 9, 3397.
- (45) Johnson, E. R.; Becke, A. D.; Sherrill, C. D.; Di Labio, G. A. *J. Chem. Phys.* **2009**, 131, 034111.
- (46) Wheeler, S. E.; Houk, K. N. *J. Chem. Theory Comput.* **2010**, 6, 395.
- (47) Perdew, J. P.; Ruzsinszky, A.; Csonka, G. A.; Vydrov, O. A.; Scuseria, G. E.; Constantin, L. I.; Zhou, X.; Burke, K. *Phys. Rev. Lett.* **2008**, 100, 136406.
- (48) Csonka, G. I.; Ruzsinszky, A.; Perdew, J. P.; Grimme, S. *J. Chem. Theory Comput.* **2008**, 4, 888.
- (49) Perdew, J. P.; Burke, K.; Ernzerhof, M. *Phys. Rev. Lett.* **1996**, 77, 3865–3868; **1997**, 78, 1396(E).
- (50) Ahlrichs, R.; Penco, R.; Scoles, G. *Chem. Phys.* **1977**, 19, 119.
- (51) Grimme, S.; Antony, J.; Schwabe, T.; Mück-Lichtenfeld, C. *Org. Biomol. Chem.* **2007**, 5, 741.
- (52) Schwabe, T.; Grimme, S. *Acc. Chem. Res.* **2008**, 41, 569.
- (53) Minenkov, Y.; Occhipinti, G.; Jensen, V. R. *J. Phys. Chem. A* **2009**, 113, 11833.
- (54) *Gaussian Development Version*, Revision H.07; Frisch, M. J.; Trucks, G. W.; Schlegel, H. B.; Scuseria, G. E.; Robb, M. A.; Cheeseman, J. R.; Scalmani, G.; Barone, V.; Mennucci, B.; Petersson, G. A.; Nakatsuji, H.; Caricato, M.; Li, X.; Hratchian, H. P.; Izmaylov, A. F.; Bloino, J.; Zheng, G.; Sonnenberg, J. L.; Hada, M.; Ehara, M.; Toyota, K.; Fukuda, R.; Hasegawa, J.; Ishida, M.; Nakajima, T.; Honda, Y.; Kitao, O.; Nakai, H.; Vreven, T.; Montgomery, J. A., Jr.; Peralta, J. E.; Ogliaro, F.; Bearpark, M.; Heyd, J. J.; Brothers, E.; Kudin, K. N.; Staroverov, V. N.; Kobayashi, R.; Normand, J.; Raghavachari, K.; Rendell, A.; Burant, J. C.; Iyengar, S. S.; Tomasi, J.; Cossi, M.; Rega, N.; Millam, J. M.; Klene, M.; Knox, J. E.; Cross, J. B.; Bakken, V.; Adamo, C.; Jaramillo, J.; Gomperts, R.; Stratmann, R. E.; Yazyev, O.; Austin, A. J.; Cammi, R.; Pomelli, C.; Ochterski, J. W.; Martin, R. L.; Morokuma, K.; Zakrzewski, V. G.; Voth, G. A.; Salvador, P.; Dannenberg, J. J.; Dapprich, S.; Parandekar, P. V.; Mayhall, N. J.; Daniels, A. D.; Farkas, O.; Foresman, J. B.; Ortiz, J. V.; Cioslowski, J.; Fox, D. J. *Gaussian, Inc.*: Wallingford, CT, 2009.
- (55) Dunning, T. H., Jr. *J. Chem. Phys.* **1989**, 90, 1007.
- (56) Krishnan, R.; Binkley, J.; Seeger, R.; Pople, J. *J. Chem. Phys.* **1980**, 72, 650.
- (57) Boys, S. F.; Bernardi, F. *Mol. Phys.* **1970**, 19, 553.
- (58) Vosko, S. H.; Wilk, L.; Nusair, M. *Can. J. Phys.* **1980**, 58, 1200–1211.
- (59) Tao, J.; Perdew, J. P.; Staroverov, V. N.; Scuseria, G. E. *Phys. Rev. Lett.* **2003**, 91, 146401.
- (60) Zhao, Y.; Truhlar, D. G. *J. Chem. Phys.* **2006**, 125, 194101.
- (61) Zhao, Y.; Truhlar, D. G. *J. Phys. Chem. A* **2006**, 110, 13126.
- (62) Spies, P.; Fröhlich, R.; Kehr, G.; Erker, G.; Grimme, S. *Chem.—Eur. J.* **2008**, 14, 333.
- (63) The Supporting Information of ref 22 considered the ground state of $\text{Mes}_2\text{P}-\text{CH}_2-\text{CH}_2-\text{B}(\text{C}_6\text{F}_5)_2$. This state has a B–P dative bond in a four-membered heterocycle. The reference reported energy differences relative to two higher-energy isomers with a broken B–P bond. Calculated energy differences between the ground state and the two bond-broken isomers were 6.8 and 7.0 kcal/mol with B97-D, and 11.3 and 10.4 kcal/mol with the more accurate spin-component-scaled⁷⁵ MP2 method.
- (64) Lynch, B. J.; Truhlar, D. G. *J. Phys. Chem. A* **2003**, 107, 8996; **2004**, 108, 1460(E).
- (65) Lynch, B. J.; Zhao, Y.; Truhlar, D. G. *J. Phys. Chem. A* **2005**, 109, 1643–1649.
- (66) Zheng, J.; Zhao, Y.; Truhlar, D. G. *J. Chem. Theory Comput.* **2009**, 5, 808.
- (67) Iglesias, E.; Sordo, T. L.; Sordo, J. A. *Chem. Phys. Lett.* **1996**, 248, 179.

- (68) Zhao, Y.; Lynch, B. J.; Truhlar, D. G. *J. Phys. Chem. A* **2004**, *108*, 2715–2719.
- (69) Curtiss, L. A.; Raghavachari, K.; Redfern, P. C.; Pople, J. A. *J. Chem. Phys.* **2000**, *112*, 7374–7382.
- (70) Zhao, Y.; Truhlar, D. A. *J. Chem. Theory Comput.* **2008**, *4*, 1849.
- (71) Antony, J.; Grimme, S. *Phys. Chem. Chem. Phys.* **2006**, *8*, 5287.
- (72) Vreven, T.; Morokuma, K. *J. Chem. Phys.* **1999**, *111*, 8799.
- (73) Curtiss, L. A.; Raghavachari, K. *Theor. Chem. Acc.* **2002**, *108*, 61.
- (74) The timings in Figure 3 are the total wall clock time in Link 502, divided by the number of SCF iterations. The calculations use “SCF=Tight, Integral(Grid=UltraFine)” and default Gaussian parameters otherwise.
- (75) Grimme, S. *J. Chem. Phys.* **2003**, *118*, 9095.

CT1000846